**16th International Symposium on Unsteady Aerodynamics**
**Aeroacoustics and Aeroelasticity of Turbomachines**
**ISUAAAT16**
**September 19th-23rd, 2022, Toledo, Spain**

# ISUAAAT16-85

## NUMERICAL INVESTIGATION OF AEROELASTICITY OF WIND TURBINES USING A NONLINEAR FREQUENCY DOMAIN SOLUTION METHOD

***Shine Win Naung*[1]*; Mohammad Rahmati*[1*]**
*[1]Department of Mechanical and Construction Engineering, Northumbria University, Newcastle upon Tyne NE1 8ST.*

*[*]Corresponding Author:* ***Mohammad Rahmati***
***mohammad.rahmati@northumbria.ac.uk***

## ABSTRACT

An extensive numerical investigation of the aeroelasticity of wind turbines is presented in the present paper. A highly efficient nonlinear frequency domain solution method is employed for this analysis. A complete wind turbine model including a tower with oscillating blades is analysed based on a relatively high amplitude of vibration. A nonlinear frequency domain solution method only requires a single blade to be modelled; however, it can capture the unsteady flow behaviour associated with blade vibration at a given inter-blade phase angle. The results revealed that the blade oscillation has an impact on the aerodynamic and aeroelastic performance of a wind turbine by producing pressure fluctuations on the pressure and suction surfaces of the blade and influencing the flow structures around the wind turbine. It is seen that the flow structures leaving from the rotor are distorted by the tower, and a combined effect of the blade oscillation and the tower leads to an unsteady and turbulent downstream wake. It is also noted that a nonlinear frequency domain solution method employed in this study is computationally efficient as it solves significantly faster than the conventional time domain methods.

Keywords: Wind turbines, aerodynamics, aeroelasticity, computational fluid dynamics (CFD), fluid-structure interaction, frequency domain method

## 1. INTRODUCTION

The generation of electricity from clean energy resources has become critical to meeting the net-zero target which requires a 100% decarbonisation of the electricity system of the UK. The UK government published a ten-point plan for a green industrial revolution, targeting net-zero greenhouse gas emissions by 2050 [1]. Among renewable energy resources, wind power has a major role in delivering the transformation to net-zero [2]. To achieve net-zero, it requires additional development of 30 GW from onshore wind alone by 2030 [3]. This significantly raises the demand for wind energy research to maximise the capacities of wind turbines.

While experiments are not always feasible, especially for large-scale wind turbines, wind power research needs to rely on numerical tools and simulations to enhance understanding of their physical behaviours and performances [4]. Various studies have been conducted to seek efficient numerical tools to perform unsteady aerodynamic simulations of turbomachines including wind turbines without requiring high computational costs and resources. The most well-known and common method in the design of wind turbines is the Blade Element Momentum (BEM) method [5]. This method couples the momentum theory and the blade element method and provides reasonable results depending on the availability of sufficient aerofoil data. The BEM method is computationally efficient, and it has mostly been adopted for the prediction of aerodynamic loads for wind turbines [6, 7]. But the BEM method is mainly based on quasi-steady assumptions, and it requires various empirical correction models such as tip loss correction, dynamic inflow and stall [8, 9], and it is often regarded as a low-fidelity model and only used in the initial design stage of modern wind turbines [10]. Furthermore, the BEM method cannot provide the flow details which makes it difficult to understand the aerodynamic flow behaviour of wind turbines.

Unlike the BEM method, vortex models and actuator-type models can provide a good insight into the wake development and flow structures around wind turbines, and these methods are applied to the aerodynamic modelling of wind turbines. Lee et al. [11] proposed an unsteady vortex-lattice method to model for the analysis of wind turbine wakes. Rodriguez et al. [12, 13] used a free-wake method for the aeroelastic modelling of offshore wind turbines, whereas Breton et al. [14] applied a prescribed-wake method to the wind turbine analysis. The main limitation of vortex models is that the viscous effects are ignored by most vortex models.

Moreover, the actuator-type methods, originally proposed by Froude [15] and Rankine [16], are also used for the analysis of rotor aerodynamics. Using an actuator type method, a rotor or a blade of a turbomachine is replaced by a disk model, known as an actuator disk method, or a line model, known as an actuator line method, with variable load distributions. These methods work in a similar way to the BEM method for the computation of aerodynamic loads. But they are now typically combined with a flow solver to solve the governing equations such as Navier-Stokes equations to analyse the wake developments. Sorensen et al. [17] carried out an unsteady aerodynamic simulation of wind turbines based on an actuator disk method and a finite difference method to solve the Navier-Stokes equations. Furthermore, an actuator line method was also used in the study of Troldborg et al. [18] for the aerodynamic analysis of wind turbines operating in the unsteady turbulent wake. Actuator-type models can provide a great insight into the turbulent wake structures behind a wind turbine with reasonable accurate aerodynamic loadings. However, similar to BEM models, they also require sufficient aerofoil data for the calculation of aerodynamic loads, whereas the computational costs are much more expensive than BEM models as it involves a flow solver to solve the flow governing equations [19].

Computational Fluid Dynamics (CFD) methods are often referred to as high-fidelity methods as they solve the governing equations. The details of flow structures can be resolved using an appropriate turbulence modelling technique. Due to advances in computing technologies, the CFD methods are now widely applied to wind turbine analyses. Liu et al. [20] established a fully coupled CFD method for the aerodynamic modelling of floating offshore wind turbines. CFD methods are typically coupled with structural models for the aeroelastic modelling of wind turbines. Wang et al. [21] proposed a coupled CFD and Finite Element Analysis (FEA) method for the analysis of wind turbine aerodynamics and aeroelasticity. Likewise, Dose et al. [22, 23] employed a coupled CFD and Computational Structural Dynamics (CSD) model to carry out the aeroelastic simulations of wind turbines. The major drawback of CFD-based methods is that they demand significantly high computational costs and resources, especially for fully unsteady simulations.

Efficient numerical tools and methods that can reduce the computational cost while maintaining the required accuracy are being developed for the modelling of aerodynamics and aero-elasticity of turbomachinery including wind turbines. Frequency domain solution methods such as the harmonic solution method of Rahmati et al. [24, 25] are found to be efficient solutions due to their capabilities of providing accurate solutions at a reasonable computational cost. Win Naung et al. [26-28] recently proposed a nonlinear frequency domain solution method for the analysis of aerodynamics and aeroelasticity of wind turbines, taking different sources of flow unsteadiness such as inflow wake and turbulences, a large amplitude of blade vibration, and rotor-tower interaction, into account. They later extended it to performing CFD simulations of two wind turbines in arrays, connected by a series of rotor-stator interfaces, and analysed the effects of the upstream wind turbine on the downstream turbine at different separation distances [29]. Extensive verification and validation of a frequency domain solution method were also carried out by Win Naung et al. [30, 31] using direct numerical simulations. It was discussed that the frequency domain method is computationally efficient without compromising the required accuracy of flow modelling and the prediction of aerodynamic loads.

This paper evaluates the impact of blade vibration in wind turbines on the stability and aeroelastic performances of wind turbines using a nonlinear frequency domain solution method, developed by the authors. A well-known test case wind turbine model is employed to perform an aeroelasticity analysis based on a modal coupling approach. Relatively high amplitude of vibration is modelled in this analysis. The tower is also included in the modelling and the effects of the tower on the unsteady flow behaviour are investigated in the present paper.

## 2. MODEL DESCRIPTION

A well-known MEXICO (Model Rotor Experiments In Controlled Conditions) wind turbine model is employed in this paper. This model has been widely used as a benchmarking model to validate various numerical codes in the literature. The details of the experiment and the wind turbine model can be found in [32-35] as well as in the authors' previous papers [26-28]. The rotor consists of three blades with a length of 2.04 m, and the diameter of the rotor is 4.5 m. The design wind speed and the rotational speeds are 15 m/s and 424.5 RPM, respectively, which corresponds to the tip speed ratio of 6.67. The blade oscillation is also integrated into the modelling and analysis of this wind turbine. A general material, Aluminium Alloy, is used to be consistent with the experiment. The modal analysis is initially performed to compute the natural frequencies and the structural mode shapes of the blade, which are then used in the flow simulation to define the blade vibration. The first natural frequency (15.611 Hz) and the mode shape are specified to be the vibration frequency and vibration mode of the blade as the first vibration mode is considered to be the fundamental source of vibration. A relatively large amplitude of 9% span, which corresponds to 9 m in a 100 m-long blade which is typically seen in modern offshore wind turbines, is defined as the vibration amplitude. The tower is also considered in the modelling to analyse the impact of the tower and the effects associated with the rotating and stationary components of a wind turbine. A schematic diagram of the MEXICO wind turbine and the physical model employed for this paper can be seen in Fig. 1.

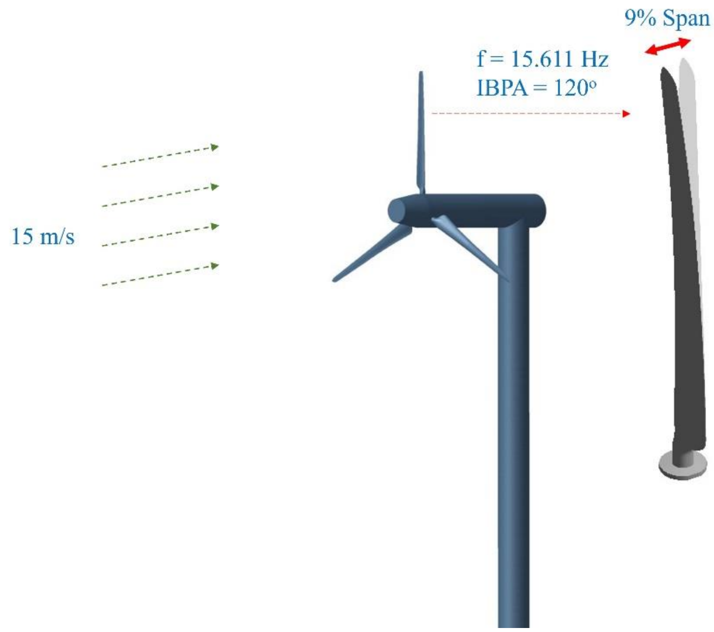


**FIGURE 1:** SCHEMATIC DIAGRAM OF THE MEXICO WIND TURBINE AND THE PHYSICAL MODEL.

## 3. METHODOLOGIES

### 3.1 Flow Governing Equations

The main objective of this work is to model and analyse the aeroelastic performances of wind turbines subject to the flutter behaviour of the rotor blades using a nonlinear frequency domain solution method. The modal coupling method is used for the modelling of fluid-structure interactions. A CFD method is used for the aerodynamic computation and an FEA method is used for the structural computation. The modal analysis is first performed in an FEA environment to compute the natural frequencies and the mode shapes, which are then imported into the flow solver. The flow is governed by the Navier-Stokes equations that are solved by a three-dimensional, pressure-based, finite volume solver. The general Navier-Stokes equations can be represented by:

$$\frac{\partial}{\partial t}\int_{Q} U dQ + \int_{A} \vec{I}_F \, . d\vec{A} + \int_{A} \vec{V}_F \, . d\vec{A} = \int_{Q} S dQ \tag{1}$$

In this equation, $Q$ is the volume, $A$ is the surface, $U$ is the vector of the flow variables, $S$ is the source term, and $\vec{I}_F$ and $\vec{V}_F$ are the inviscid and viscous flux vectors, respectively. The Navier-~Stokes equations can be simply written as:

$$\frac{\partial}{\partial t}(U) = R(U) \tag{2}$$

where R is the lumped residual and source term. A Reynolds Averaged Navier-Stokes (RANS) approach is used for the CFD simulation. The Spalart-Allmaras turbulence model is employed for turbulence modelling.

A nonlinear frequency domain solution method is employed for the modelling and simulation of the aeroelasticity of wind turbines. With the frequency domain solution method, the conservative flow variables $U$ can be represented by the Fourier series for a prescribed fundamental frequency, ω, and specified number of harmonics, m, as expressed in Eq. (3) [26, 27].

$$U = \bar{U} + \sum_{m=1}^{M} [\alpha_U \sin(m\omega t) + \beta_U \cos(m\omega t)] \tag{3}$$

In this equation, $\bar{U}$ is the time-averaged parameter, and $\alpha_U$ and $\beta_U$ are Fourier coefficients. Substituting Eq. (3) into Eq. (2) will lead to a set of new unsteady Navier-Stokes equations. Using the nonlinear frequency domain solution method, the unsteady period is equally divided into $N = (2m+1)$ time levels and the system of nonlinear equations coupling all $N$ time levels is solved iteratively. The fundamental frequency ($1^{st}$ harmonic) is only considered in this study.

### 3.2 Computational Domain and Grid

The three-dimensional computational domain and grid employed in this study are shown in Fig. 2. Separate domains for the rotor and the tower are created. They are meshed separately and connected by a rotor-stator interface to model the complete wind turbine. A rounded O4H topology is used to generate the structured grid for both domains presented in this figure. An O-mesh is used for the skin block surrounding either blade or tower, whereas an H-mesh is used for the rest of the blocks. The first cell layer thickness is $1 \times 10^{-5}$ meters which ensures that the $y^+$ value is less than one to adequately resolve the boundary layer flow. One of the great benefits of the nonlinear frequency domain solution method is that it only requires a single rotor blade (120° domain), and the flow harmonics can be phase-shifted between periodic boundaries. Unlike this method, the typical time-domain solution method requires all three blades (360° domain). The tower is modelled using a 360° domain in both methods. The inflow and outflow of the computational domains are located 4R upstream and 8R downstream of the rotor plane, respectively, where R is the rotor radius. The far-field boundary is placed 3R from the origin of the rotor plane. The generated rotor (120°) domain and the tower (360°) domain consists of $4.5 \times 10^6$ and $14 \times 10^6$ elements, respectively.

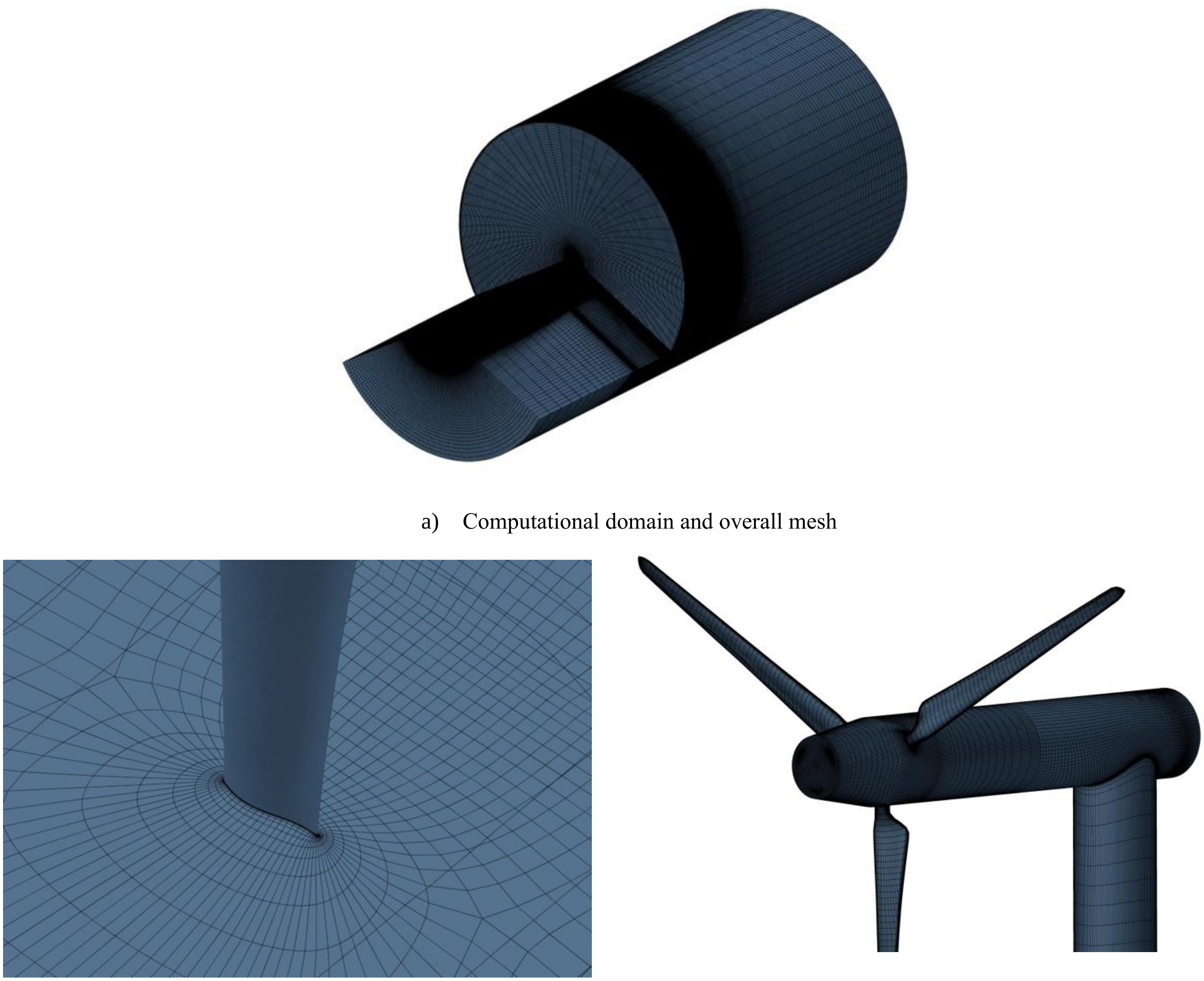

a) Computational domain and overall mesh

b) Blade-to-blade mesh

c) 3D solid mesh

**FIGURE 2:** COMPUTATIONAL DOMAIN AND GRID GENERATED.

### 3.3 Boundary Conditions and Numerical Scheme

A no-slip wall boundary condition is specified on the surfaces of the rotor blade, hub and tower, and an external boundary condition is defined to treat the far-field boundaries. A periodic boundary condition is implemented in the frequency domain solution to account for all three blades in the simulation, whereas a full wheel of the rotor with all three blades is used in the time domain solution. A non-matching rotor-stator interfaced is employed to connect the rotor domain to the tower domain to simulate the complete wind turbine model. A non-linear harmonic method is used for the rotor-stator interface with the frequency domain solution method, whereas a sliding-plane method is used with the time domain solution method. In the frequency domain method, the time-mean value and the harmonic components of the conservative flow variables are phase-shifted across the rotor-stator interface and between periodic boundaries by a given inter-blade phase angle. On the other hand, in the time domain solution method, the instantaneous flow data are exchanged across the rotor-stator interface at each time step using a direct local interpolation method.

A central scheme is used for the spatial discretization and a four-step Runge-Kutta scheme is employed for the temporal discretization of the governing equations. A steady-state analysis is first performed and specified to be the initial condition in the unsteady simulation for faster and stable convergence. For the modelling of fluid and structure interactions, the modal coupling method is used. In this method, the modal analysis is performed to calculate the natural frequencies and the structural mode shapes of the blade before the flow simulation. The natural frequencies and the mode shapes are imported into the flow simulation to facilitate the blade vibration. A detailed description of the modal coupling method and the frequency domain method can be found in [26-28].

## 4 RESULTS AND DISCUSSION

First, the CFD model is validated against the experiment in terms of the steady pressure coefficient distributions on the blade surfaces at different sections. The comparisons are provided at 60% and 92% of the blade span sections (see Fig. 3). The detailed comparisons between the experiment and simulations at all other sections of the blade can be found in the previous papers of the authors [26, 27]. A close agreement is obtained between the experiment and the simulation ensuring that the numerical model employed in this study is valid.

An unsteady simulation of a complete wind turbine model is performed in which all three blades are vibrating at their first natural frequency (15.611 Hz) with an inter-blade phase angle of 120°. The aerodynamic and aeroelastic behaviour of the wind turbine due to the interaction between the transient flow and the turbine structures with oscillating blades are investigated in this analysis. The proposed nonlinear frequency domain solution method is employed to perform an aeroelasticity simulation. The fully unsteady simulation in the time domain is also conducted to validate the results from the frequency domain solution. The displacement contours of the wind turbine rotor blades exported from the frequency domain solution are presented in Fig. 4. It is seen that there is a phase-shift between the blades by a 120° as specified, and the frequency domain solution method only requires a single blade to model this behaviour.

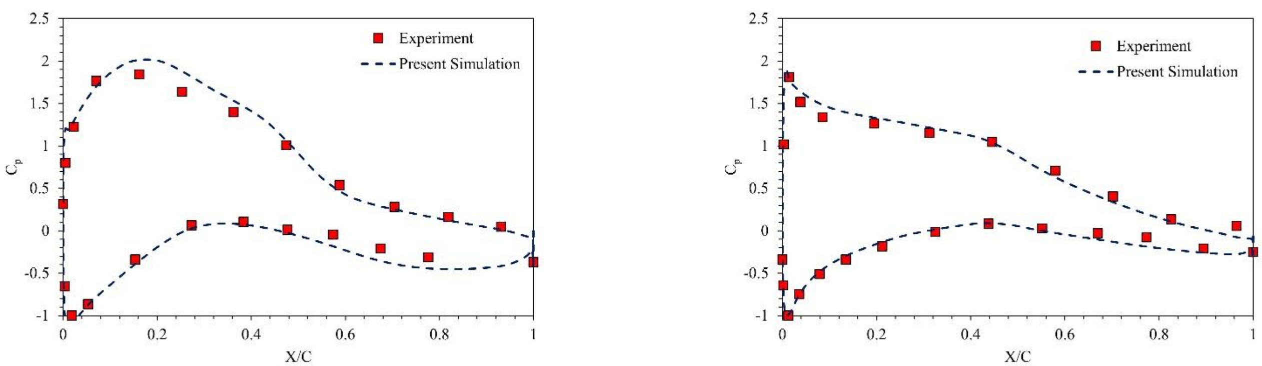


a) 60% span  b) 92% span

**FIGURE 3:** STEADY PRESSURE COEFFICIENT ($C_P$) DISTRIBUTION OVER THE BLADE SURFACES.

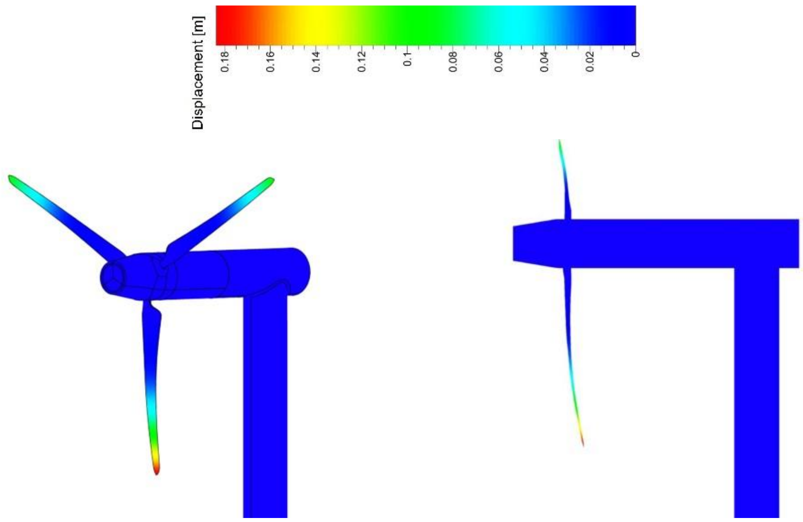


a) 3D view b) Side view

**FIGURE 4:** DISPLACEMENT CONTOUR OF THE WIND TURBINE ROTOR BLADES.

The blade vibration triggers unsteady pressure fluctuations and pressure bubbles over the blade which can be represented by an unsteady pressure amplitude and phase angle distribution. Figure 5 compares the unsteady pressure amplitude coefficient and unsteady pressure phase angle distribution on the pressure and suction surfaces of the blade at 30%, 50% and 90% span sections. It is shown that they agree well with each other which indicates that the frequency domain solution method captures unsteady distribution on the blade due to its vibration very well. Results show that the unsteady pressure fluctuations are very high at the leading edge of the blade aerofoil where the blade interacts with the incoming flow. The unsteady pressure phase angle varies within ±180°. Both unsteady pressure amplitude and phase angle variations are slightly more pronounced in the blade root region.

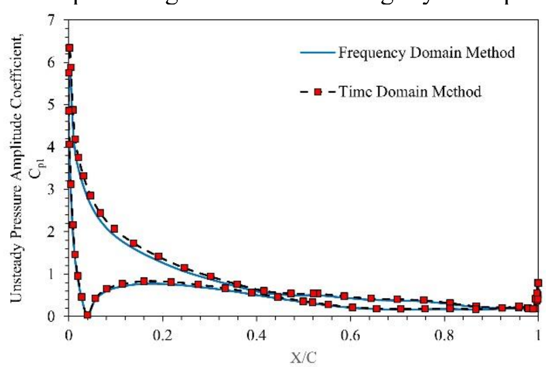


a) $C_{p1}$, 30% span

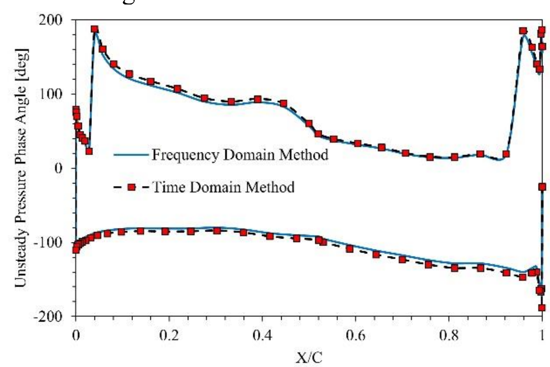


b) Phase angle, 30% span

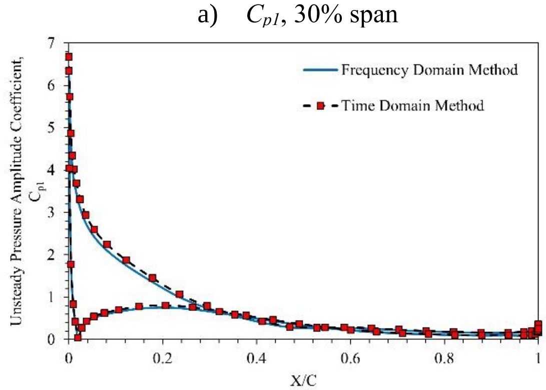


c) $C_{p1}$, 50% span

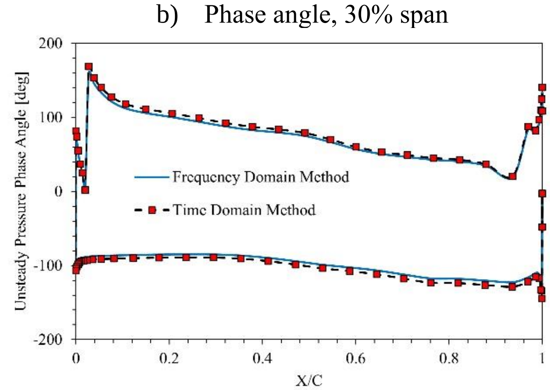


d) Phase angle, 50% span

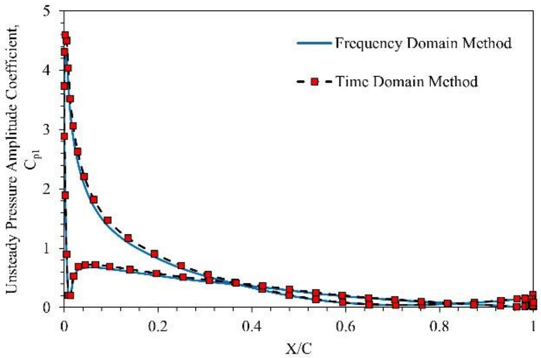


e) $C_{p1}$, 90% span

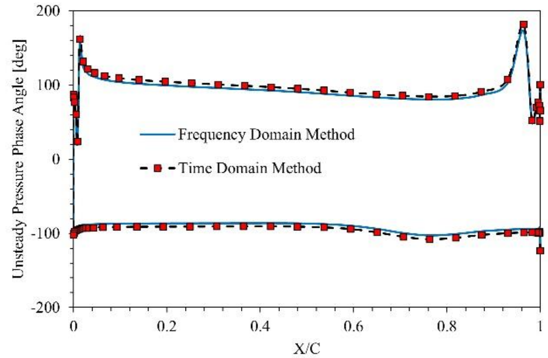


f) Phase angle, 90% span

**FIGURE 5:** UNSTEADY PRESSURE AMPLITUDE COEFFICIENT ($C_{P1}$) AND PHASE ANGLE DISTRIBUTION ON THE BLADE.

Figure 6 presents the instantaneous pressure contours on the pressure and suction surfaces of the wind turbine rotor blades. It can be observed that the pressure distribution over the blade is similar in all three blades. But one of the blades has a noticeably higher pressure on the pressure surface and lower pressure on the suction surfaces around the blade tip than the remaining two blades. This is related to the blade oscillation with an inter-blade phase angle, which results in each blade experiencing different pressure distribution on both surfaces. The frequency domain solution method captures this behaviour without requiring all three blades.

Relative velocity vectors around the blade are plotted in Fig. 7. The contours plotted are coloured by the static pressure. The relation between the pressure distribution and velocity vectors can be visualised in this figure. As the relative wind velocity interacts with the blade aerofoil, the velocity vectors are diverted from the leading edge and distributed over both the pressure and suction surface of the blade. It is seen in this figure that the velocity distribution is higher on the suction surface. As the pressure and velocity are indirectly proportional, the pressure is found to be higher on the pressure surface, especially around the leading edge and the trailing edge of the blade aerofoil. As the blade vibration presents, the motion of the blade structure only exacerbates the distortion of velocity vectors, which leads to both pressure and velocity fluctuations over the blade surfaces.

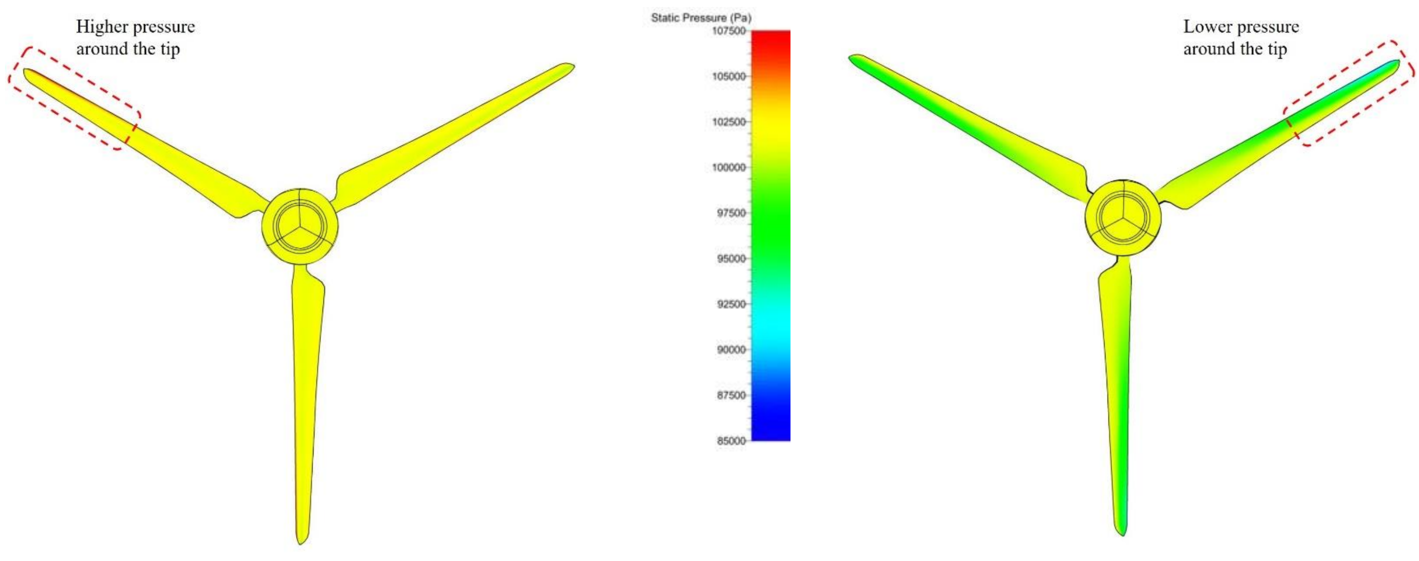


a) Pressure side

b) Suction side

**FIGURE 6:** PRESSURE CONTOUR ON THE PRESSURE AND SUCTION SURFACES OF THE BLADE.

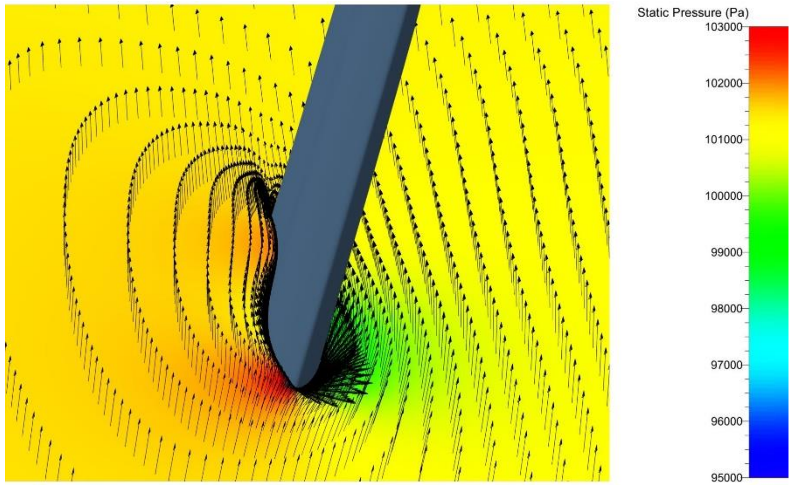


**FIGURE 7:** VELOCITY VECTORS AROUND THE WIND TURBINE BLADE.

The presence of the tower affects the aerodynamic flow field around the wind turbine. The velocity field around the wind turbine and the development of wake structures are demonstrated in Fig. 8. The generation of tip vorticity can be observed in this figure. It can be noted that the blade oscillation intensifies the vortex generation process. As the kinetic energy in the wind is captured by the wind turbine rotor, the flow past through the rotor has a significantly lower velocity magnitude. The flow is further distorted by the tower, and some vortex structures are developed along the length of the tower. The generation of hub vortices can also be seen in this figure, which then combines with those of the rotor blades. The structural vibration of the blades adds more disturbances and energy to the flow around the blade, which eventually affects the downstream wake region.

The unsteady flow due to the relation between the rotating and stationary components of the wind turbine can be observed in Fig. 9 It shows the development of the tip vorticity from the blades and the flow streamlines around the wind turbine. The generation of tip vorticity is activated by the rotation of the wind turbine rotor, and the diffusion and advection process of vorticity can be identified in this figure. The vortex structures generated from the blade are deformed when interacting with the tower, which leads to an increase in the turbulence level and additional wake structures in the downstream flow. The development of vorticity along the tower structure is also seen in Fig 9 (a). In Fig. 9 (b), the velocity streamlines past through the blades are influenced by the tower structure, and some of the velocity streamlines attach to the tower contributing to the development of the tower vortices. The flow interaction between the rotor and the tower adds flow disturbances which lead to unstable and disoriented flow streamlines in the wake region.

All the results presented in this paper are obtained from the frequency domain solution method. Although a single blade with periodic boundaries is used in the simulation, this method can capture the behaviour of the unsteady flow associated with the interaction between the blades by the use of an inter-blade phase angle. This is one of the great benefits of this method as the conventional time-domain method requires all three blades to resolve this flow behaviour.

The present numerical investigations are performed on a 16-core computer with a 3.40 GHz Intel (R) Core (TM) i5-7500 CPU, and it takes around 18 hours with the nonlinear frequency domain solution method. However, it takes more than 240 hours with the time domain solution method. The proposed frequency domain solution method reduces the computational cost by one to two orders of magnitude, without compromising the required level of accuracy, compared to the conventional time domain solution method. Therefore, it can be noted that the frequency domain solution method is an effective and efficient alternative to the traditional time-domain methods for the modelling of the aeroelasticity of wind turbines.

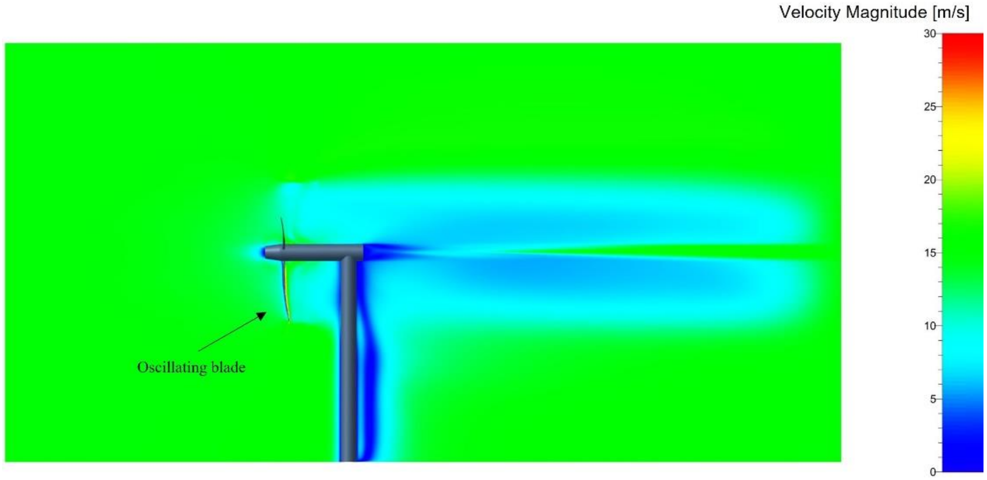


**FIGURE 8:** DEVELOPMENT OF THE VELOCITY FIELD AROUND THE WIND TURBINE.

a) Vorticity

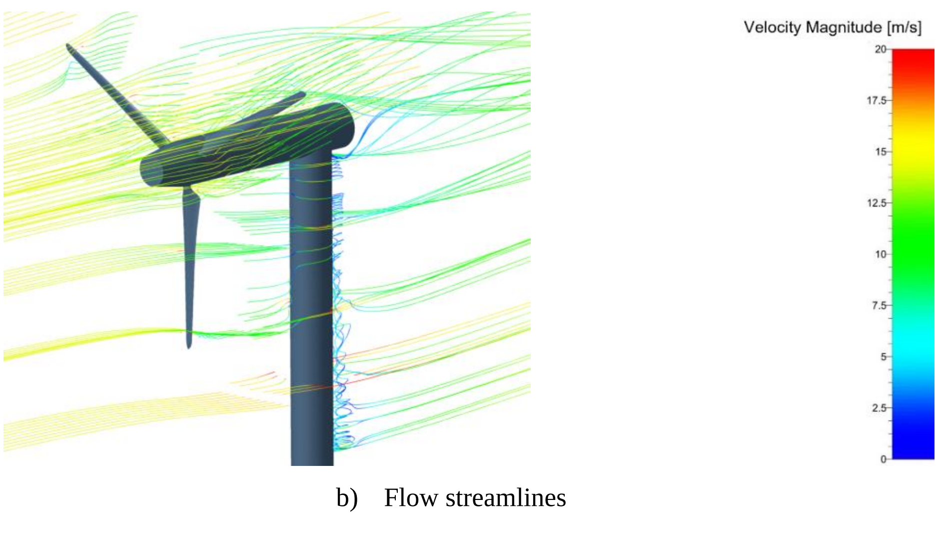


b) Flow streamlines

**FIGURE 9:** DEVELOPMENT OF TIP VORTICITY AND FLOW STREAMLINES AROUND THE WIND TURBINE.

## 5 CONCLUSION

The aeroelasticity modelling and analysis of a complete wind turbine model including a tower are presented in this paper. A nonlinear frequency domain method is employed for this analysis. The validations against the experiment and the time domain solution methods for the prediction of steady and unsteady pressure distribution over the blade surfaces confirm the reliability of the frequency domain solution method as an excellent agreement is obtained between different methods. Results obtained demonstrate the effect of blade vibration on the aerodynamic performance of a wind turbine. It is found that blade vibration causes pressure fluctuation on the blade surfaces which is also directly associated with the velocity vectors applied to the blade aerofoil. The interaction between the unsteady flow and the oscillation of the blade influences the development of tip vorticity and adds more disturbances to the wake. Furthermore, the tip vortices and the flow leaving from the rotor are distorted by the tower, leaving some vortex structures attached to the tower structure as well as adding more turbulence to the downstream wake. This paper also highlights that the frequency domain solution method is not only computationally efficient but also very accurate, and this can be a great benefit for the modelling and simulation of the aeroelasticity of wind turbines, which usually demand a high computational cost with a time domain method.

## ACKNOWLEDGEMENTS

The authors would like to acknowledge the financial support received from the Engineering and Physical Sciences Research Council of the UK (EPSRC EP/R010633/1).

## MAIN REFERENCES

[1] UK Government, 2020, "The Ten Point Plan for a Green Industrial Revolution," https://www.gov.uk/government/publications/the-ten-point-plan-for-a-green-industrial-revolution/title.
[2] UK Government, 2021, "Net Zero Strategy," https://assets.publishing.service.gov.uk/government/uploads/system/uploads/attachment_data/file/1033990/net-zero-strategy-beis.pdf.
[3] RenewableUK, 2021, "RenewableUK Onshore Wind Prospectus," https://www.renewableuk.com/news/583052/RenewableUK-Onshore-Wind-Prospectus-.htm.
[4] Micallef, D., and Rezaeiha, A., 2021, "Floating offshore wind turbine aerodynamics: Trends and future challenges," Renewable and Sustainable Energy Reviews, 152, p. 111696.
[5] Erich Hau, 2006, Wind Turbines: Fundamentals, Technologies, Application, Economics, Springer-Verlag Berlin Heidelberg.
[6] Wang, Q., Wang, J., Chen, J., Luo, S., and Sun, J., 2015, "Aerodynamic shape optimized design for wind turbine blade using new airfoil series," Journal of Mechanical Science and Technology, 29(7), pp. 2871-2882.
[7] Yang, Y., Bashir, M., Michailides, C., Li, C., and Wang, J., 2020, "Development and application of an aero-hydro-servo-elastic coupling framework for analysis of floating offshore wind turbines," Renewable Energy, 161, pp. 606-625.
[8] Buhl, M. L., 2005, "A New Empirical Relationship between Thrust Coefficient and Induction Factor for the Turbulent Windmill State " No. NREL/TP-500-36834, National Renewable Energy Laboratory, Golden, Colorado.
[9] Dowler, J. L., and Schmitz, S., 2015, "A solution-based stall delay model for horizontal-axis wind turbines," Wind Energy, 18(10), pp. 1793-1813.
[10] Otter, A., Murphy, J., Pakrashi, V., Robertson, A., and Desmond, C., 2022, "A review of modelling techniques for floating offshore wind turbines," Wind Energy, 25(5), pp. 831-857.
[11] Lee, H., and Lee, D.-J., 2019, "Numerical investigation of the aerodynamics and wake structures of horizontal axis wind turbines by using nonlinear vortex lattice method," Renewable Energy, 132, pp. 1121-1133.
[12] Rodriguez, S. N., and Jaworski, J. W., 2019, "Strongly-coupled aeroelastic free-vortex wake framework for floating offshore wind turbine rotors. Part 1: Numerical framework," Renewable Energy, 141, pp. 1127-1145.
[13] Rodriguez, S. N., and Jaworski, J. W., 2020, "Strongly-coupled aeroelastic free-vortex wake framework for floating offshore wind turbine rotors. Part 2: Application," Renewable Energy, 149, pp. 1018-1031.
[14] Breton, S.-P., Coton, F. N., and Moe, G., 2008, "A study on rotational effects and different stall delay models using a prescribed wake vortex scheme and NREL phase VI experiment data," Wind Energy, 11(5), pp. 459-482.
[15] Froude, R. E., 1889, "On the Part Played in Propulsion by Differences of Fluid Pressure," Trans. Inst. Naval Architects, 30, p. 390.
[16] Rankine, W. J. M., 1865, "On the Mechanical Principles of the Action of Propellers," Transactions of the Institution of Naval Architects, 6.
[17] Sørensen, J. N., Shen, W. Z., and Munduate, X., 1998, "Analysis of wake states by a full-field actuator disc model," Wind Energy, 1(2), pp. 73-88.
[18] Troldborg, N., Sørensen, J. N., and Mikkelsen, R., 2007, "Actuator Line Simulation of Wake of Wind Turbine Operating in Turbulent Inflow," Journal of Physics: Conference Series, 75, p. 012063.
[19] Wang, L., Liu, X., and Kolios, A., 2016, "State of the art in the aeroelasticity of wind turbine blades: Aeroelastic modelling," Renewable and Sustainable Energy Reviews, 64, pp. 195-210.

[20] Liu, Y., Xiao, Q., Incecik, A., Peyrard, C., and Wan, D., 2017, "Establishing a fully coupled CFD analysis tool for floating offshore wind turbines," Renewable Energy, 112, pp. 280-301.
[21] Wang, L., Quant, R., and Kolios, A., 2016, "Fluid structure interaction modelling of horizontal-axis wind turbine blades based on CFD and FEA," Journal of Wind Engineering and Industrial Aerodynamics, 158, pp. 11-25.
[22] Dose, B., Rahimi, H., Herráez, I., Stoevesandt, B., and Peinke, J., 2018, "Fluid-structure coupled computations of the NREL 5 MW wind turbine by means of CFD," Renewable Energy, 129, pp. 591-605.
[23] Dose, B., Rahimi, H., Stoevesandt, B., and Peinke, J., 2020, "Fluid-structure coupled investigations of the NREL 5 MW wind turbine for two downwind configurations," Renewable Energy, 146, pp. 1113-1123.
[24] Rahmati, M. T., He, L., and Li, Y. S., 2015, "The Blade Profile Orientations Effects on the Aeromechanics of Multirow Turbomachines," Journal of Engineering for Gas Turbines and Power, 138(6), p. 062606.
[25] Rahmati, M. T., He, L., Wang, D. X., Li, Y. S., Wells, R. G., and Krishnababu, S. K., 2013, "Nonlinear Time and Frequency Domain Methods for Multirow Aeromechanical Analysis," Journal of Turbomachinery, 136(4), p. 041010.
[26] Win Naung, S., Rahmati, M., and Farokhi, H., 2021, "Nonlinear frequency domain solution method for aerodynamic and aeromechanical analysis of wind turbines," Renewable Energy, 167, pp. 66-81.
[27] Win Naung, S., Rahmati, M., and Farokhi, H., 2021, "Aeromechanical Analysis of a Complete Wind Turbine Using Nonlinear Frequency Domain Solution Method," Journal of Engineering for Gas Turbines and Power, 143(1), p. 011018.
[28] Naung, S. W., Nakhchi, M. E., and Rahmati, M., 2021, "An Experimental and Numerical Study on the Aerodynamic Performance of Vibrating Wind Turbine Blade with Frequency-Domain Method," Journal of Applied and Computational Mechanics, 7(3), pp. 1737-1750.
[29] Win Naung, S., Nakhchi, M. E., and Rahmati, M., 2021, "High-fidelity CFD simulations of two wind turbines in arrays using nonlinear frequency domain solution method," Renewable Energy, 174, pp. 984-1005.
[30] Win Naung, S., Nakhchi, M. E., and Rahmati, M., 2021, "Prediction of flutter effects on transient flow structure and aeroelasticity of low-pressure turbine cascade using direct numerical simulations," Aerospace Science and Technology, 119, p. 107151.
[31] Win Naung, S., Rahmati, M., and Farokhi, H., 2021, "Direct Numerical Simulation of Interaction between Transient Flow and Blade Structure in a Modern Low-Pressure Turbine," International Journal of Mechanical Sciences, 192, p. 106104.
[32] Schepers, J., Boorsma, K., Cho, T., Gomez-Iradi, S., Schaffarczyk, P., Jeromin, A., Shen, W., Lutz, T., Meister, K., and Stoevesandt, B., 2012, "Final report of IEA Task 29, Mexnext (Phase 1): Analysis of Mexico wind tunnel measurements Tech. rep," ECN-E–12-004 ECN URL http://www.ecn.nl/publications/ECN-E--12-004.
[33] Schepers, J., and Snel, H., 2007, "Model experiments in controlled conditions, final report," ECN, ECN-E-07-042, Petten, the Netherlands.
[34] Schepers, J. G., Boorsma, K., and Munduate, X., 2014, "Final Results from Mexnext-I: Analysis of detailed aerodynamic measurements on a 4.5 m diameter rotor placed in the large German Dutch Wind Tunnel DNW," Journal of Physics: Conference Series, 555, p. 012089.
[35] Snel, H., Schepers, J., and Pascal, L., "First results from Mexnext: Analysis of detailed aerodynamic measurements on a 4.5 diameter rotor placed in the large German Dutch Wind Tunnel DNW," Proc. European Wind Energy Conference and Exhibition (EWEC), Warsaw, Poland, 20-23 april 2010., ECN.